

FineGrasp: Towards Robust Grasping for Delicate Objects

Yun Du*, Mengao Zhao*, Tianwei Lin, Yiwei Jin, Chaodong Huang, Zhizhong Su

Abstract—Recent advancements in robotic grasping have led to its integration as a core module in many manipulation systems. For instance, language-driven semantic segmentation enables the grasping of any designated object or object part. However, existing methods often struggle to generate feasible grasp poses for small objects or delicate components, potentially causing the entire pipeline to fail. To address this issue, we propose a novel grasping method, FineGrasp, which introduces improvements in three key aspects. First, we introduce multiple network modifications to enhance the model’s ability to handle delicate regions. Second, we address the issue of label imbalance and propose a refined graspness label normalization strategy. Third, we introduce a new simulated grasp dataset and show that mixed sim-to-real training further improves grasp performance. Experimental results show significant improvements, especially in grasping small objects, and confirm the effectiveness of our system in semantic grasping. Code will be available at [robo_orchard_lab/finegrasp](https://github.com/robo_orchard_lab/finegrasp).

I. INTRODUCTION

As one of the most frequently used end-effector designs for robotic arms, the two-finger parallel grippers have driven the development of dedicated 6-DoF grasp detection task. Recent data-driven methods [1], [2], [3] have demonstrated remarkable performance, making them a fundamental component of many robotic manipulation systems. As shown in Fig. 1, a prevalent framework integrates the grasp detection module with a semantic reasoning module (e.g., GPT-4o, SAM), which generates masks to filter grasp poses for objects specified by language commands. This semantic grasping capability enables a variety of tasks, including task-oriented grasping [4] and part grasping [5].

Existing grasping methods [1], [3] have demonstrated robust performance for various objects with regular shapes and size, achieving an average grasp success rate exceeding 90%. However, as illustrated in Fig. 2(a), our implementation of the semantic grasping system reveals that the grasp model occasionally fails to generate feasible grasp poses for small objects or small parts of medium and large objects, leading to the failure of overall system. In [6], the scale of grasp pose is defined as the minimum width between the gripper’s fingers. Accordingly, delicate grasping issues can be attributed to small-scale grasp poses.

Why do existing methods struggle with small-scale grasp pose estimation? We believe the key issue is that during training, networks tend to focus on larger, easier-to-grasp objects in complex scenes, leading to the neglect of finer objects. Prior work [6] discussed this scale imbalance problem, and addressed them by incorporating multi-scale features, scale-aware weighted loss, and explicit balanced sampling via an

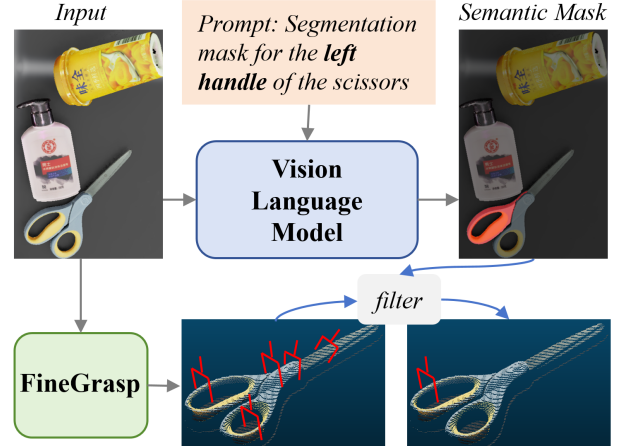


Fig. 1. Overview of a common semantic grasping framework. First, a pre-trained Vision-Language Model (VLM) is utilized to locate the desired (part of) object. Next, a point-cloud based grasping module generates the corresponding grasp poses. The primary challenge here lies in the difficulty of generating grasp poses for small objects and delicate components.

object segmentation network during inference. However, despite their initial effectiveness, these improvements are now insufficient and come with added computational overhead.

In this work, we propose a novel method **FineGrasp**, to address these challenges with three key improvements. **First**, existing methods select sparse points (e.g., 1024) from the dense point cloud based on graspability scores for grasp poses estimation. However, as shown in Fig. 2(b), global normalization of graspability labels often suppresses those of small objects, making them harder to learn. To overcome this, we introduce a new strategy that normalizes labels within each object first. This ensures that small objects receive effective supervision during training, and eliminates the need for a segmentation network during inference. **Second**, we enhance existing methods [3], [6] by introducing a multi-range attention module that extracts and fuses multi-scale features around candidate sample points via attention, allowing the model to learn scale-specific weights. We also integrate object surface normals as an auxiliary input to the grasping model, leveraging their strong correlation with optimal grasping directions to improve the network’s accuracy in orientation estimation. **Third**, depth sensor noise may lead to small objects being overlooked during training. To address this, we create supplementary simulation scenes using assets from GraspNet[1], which are combined with real data for mixed training. This strategy effectively improves overall performance. In summary, our contributions are as follows:

- We propose FineGrasp, a novel method that improves

* These authors contributed equally.
All authors are with Horizon Robotics.



Fig. 2. Illustrating the challenges of delicate object grasping based on EconomicGrasp: (a) Two typical failure scenarios: the left image shows the model failing to generate a usable grasp pose for small objects in a cluttered scene, while the right image shows poor pose quality, leading to potential failure. (b) Issues in graspness ground truth generation: the middle image shows ground truth after cross-object normalization, where scissors are ignored. The right image shows our strategy, normalizing within each object first to ensure consistent scoring across objects.

grasp pose accuracy for fine objects, demonstrating significant performance gains in experiment.

- We address the fine object grasping problem by introducing a new graspability ground truth generation strategy and several model improvements.
- We create an extended simulation dataset for GraspNet, using mixed training to enhance performance.
- We introduce a VLM-based semantic grasping framework to validate the effectiveness of our method.

II. RELATED WORK

A. 6-DoF Grasp Pose Detection

The 6-DoF grasp pose detection task revolves around two fundamental questions: "Where to grasp?" and "How to grasp?" Accordingly, most existing methods adopt a two-stage prediction pipeline — first, point sampling is used to identify graspable regions, followed by grasp pose prediction in the second stage. GSNet [7] introduced a graspness prediction task during the point sampling phase, enabling the model to more effectively identify graspable regions in cluttered scenes. To tackle scale imbalance, Scale Balanced Grasp [6] proposed an object-balanced sampling strategy using an auxiliary segmentation network, which significantly improves performance on small-scale grasps. Additionally, EconomicGrasp [3] identified dense supervision as a bottleneck in existing grasp models and proposed an economic supervision paradigm, achieving superior grasp performance with reduced computational cost.

B. Grasp Datasets

GraspNet-1Billion [1] is the most extensively utilized dataset for two-finger gripper grasps. It comprises 190 cluttered scenes constructed in real-world environments. A robotic arm equipped with an RGB-D sensor was employed to capture images from various perspectives, while the 6-DoF grasp poses were acquired through analytical computation of force closure. Nevertheless, data collection in real-world settings is inherently time-consuming and challenging, which hinders efforts to achieve large-scale expansion. As a result, certain methodologies advocate for the synthesis of grasp data within a simulation environment. For example, SimGrasp [8] introduced an approach-based sampling scheme coupled with dynamic evaluation in Isaac Sim simulator

[9] to generate grasping labels, and encompasses a substantial number of open-source assets. Furthermore, several methodologies extend this into the domain of dexterous hand grasping, such as DexGraspNet 2.0 [10].

C. Grasp Model in robotic manipulation

As a fundamental component of real-world robotic manipulation, various approaches have been developed to integrate grasp models into systems, aiming to improve efficiency and precision in object handling. OK-Robot [11] proposed a pick-and-drop solution for real-world applications by integrating VLMs for object detection, utilizing navigation primitives for movement, and employing grasping primitives for object manipulation. In this framework, AnyGrasp [2] was used to generate grasp poses. CoPa [4] leveraged the common sense knowledge embedded within foundation models to enable the task-relevant object manipulation and utilized GraspNet [1] as a key grasping module to generate 6-DOF grasp poses. To enable manipulation in unstructured environments, OmniManip [12] proposed an object-centric primitives framework to better utilize VLMs, where AnyGrasp [2] is employed.

III. METHOD

In this section, we present our method in detail. First, in Sec. III-A, we define 6-DoF grasp detection and outline the typical framework of existing grasp models. Next, in Sec. III-B, we introduce our model improvements, including intra-instance graspness label normalization strategy, multi-range attention module, and normal prior. In Sec. III-C, we describe the process of constructing our SimGraspNet dataset. Finally, in Sec. III-D, we introduce our semantic grasping solution, which leverages the capabilities of the VLM model for improved applicability in real-world scenarios.

A. Preliminary

Consistent with previous studies, we address the challenge of 6-DoF grasp detection for parallel grippers in cluttered scenes, utilizing a single-view RGBD image as input. The grasp pose is represented as $g = (x, y, z, \theta, \gamma, \beta, w)$, where (x, y, z) denotes the center of grasp, w is the grasp width and (θ, γ, β) is the intrinsic rotation as Euler angles.

Typical grasp models [1], [3] are generally comprised of three integral modules. (1) Initially, a 3D convolutional backbone extracts geometric features from the input point

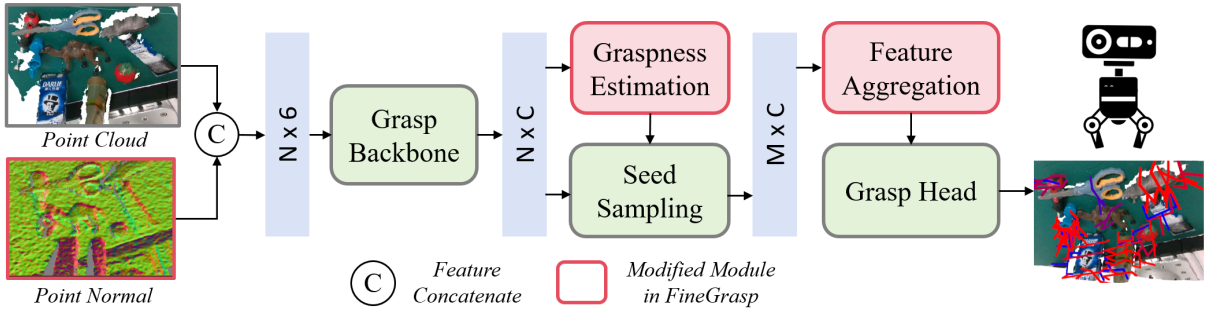


Fig. 3. Overall framework of our proposed FineGrasp. Based on EconomicGrasp [3], we introduce three key improvements: (1) Instance-normalized graspness labels to better balance different objects and ensure delicate objects are not overlooked during seed sampling; (2) Multi-range feature attention module more effective aggregation of multi-scale features. (3) Normal prior as an input to guide the network in identifying the optimal grasping orientation.

cloud, while an MLP block estimates each point’s graspability. We then select K points based on this graspability. (2) Subsequently, for each sampled point, an MLP block selects the optimal view, and the cylinder grouping module arranges local geometric features accordingly within a cylindrical space. (3) Finally, an MLP block forecasts the grasp scores, grasp depths, as well as the grasp widths for each grouping.

EconomicGrasp [3] further introduces an economic supervision paradigm, optimizing label selection and training efficiency to overcome the dense supervision bottleneck. Building upon this strong baseline, we have undertaken efforts to improve the grasp performance of delicate objects.

B. Grasp Model

Instance-Norm Graspness. As previously discussed, identifying graspable regions is crucial for the success of grasping methods. While [7] suggests that scene-level graspness prediction enhances the selection of suitable seed points, we identify two key limitations: (1) Grasp poses on delicate objects are often penalized for collisions, leading to artificially low graspness scores; (2) Scene-level normalization applies a uniform scaling across all objects, disregarding inter-object variations. This global suppression disproportionately lowers the scores of small objects, further hindering their learning.

$$\tilde{S}'_P = \left\{ \frac{\tilde{s}_p^c - \min(\tilde{S}_p^c)}{\max(\tilde{S}_p^c) - \min(\tilde{S}_p^c)} \mid c \in \mathcal{C} \right\} \quad (1)$$

$$S_P = \left\{ \frac{\tilde{s}_p^i - \min(\tilde{S}'_p)}{\max(\tilde{S}'_p) - \min(\tilde{S}'_p)} \mid i = 1, \dots, N \right\} \quad (2)$$

To address these issues, we introduce Instance-Normal Graspness, which aims to balance the learning of graspable regions across objects of different sizes. Following the Graspness generation process of GSNet [7], we obtain graspness scores for each of N points in the scene, indicating their graspability. GSNet uses global scene-level normalization for graspable supervision. In contrast, we first normalize graspness scores within each category c to highlight graspable areas within objects. Here, \mathcal{C} is the set of object categories, and \tilde{s}_p^c denotes the graspness score (with dimension $N_c \times 1$) for points in category c , where N_c is the number of points

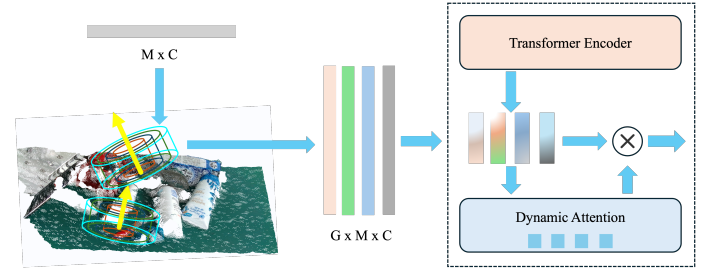


Fig. 4. Point features are aggregated across multiple ranges through a Transformer encoder, enabling cross-scale feature interaction. Adaptive fusion weights dynamically combine these features, facilitating grasp pose learning for varying sizes.

in the category. This instance-level normalization is shown in Eq.1. Finally, we apply the scene-level normalization to obtain the final scene-level graspness S_P as shown in Eq.2. **Multi-range Attention.** The graspability of an object is highly correlated with the features within its local surroundings. Therefore, for feature aggregation of each candidate seed point, it is common practice to aggregate features within a defined receptive field using cylinder grouping. Scale-Balance-Grasp [6] explored multi-scale feature aggregation by employing multiple receptive fields. Building on this, we introduce a Multi-Range Attention (MRA) mechanism that enables dynamic cross-scale feature interaction, further enhancing feature representation for grasping tasks.

As shown in Fig.3, after passing through the grasp backbone and seed sampling module, the point cloud yields features with a dimension of $M \times C$, where M and C represent the sample point number and feature dimension respectively. We set G radius ranges and apply cylinder grouping for local feature aggregation. The cylinders are oriented along the view direction, producing a multi-range feature $X \in \mathbb{R}^{G \times M \times C}$.

$$F = \text{TransformerEncoder}(X) \quad (3)$$

$$O = \sum_{g=1}^G F_g \odot \text{softmax}(W F_g) \quad (4)$$

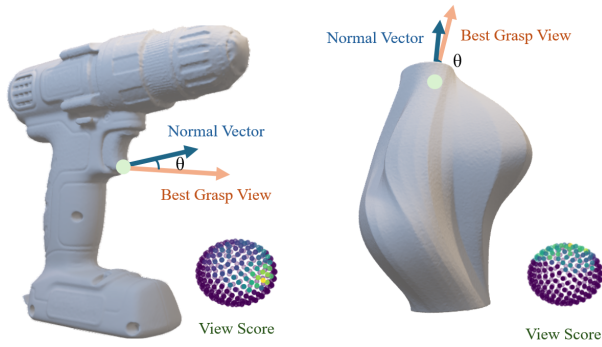


Fig. 5. The force closure score distribution in GraspNet1B exhibits a view-dependent bias, the normal vector provides a approaching prior for high-quality grasping poses regression

This feature X undergo dimensional transformation and contextual encoding through a Transformer module (Eq.3), producing latent representations that capture inter-group dependencies. Moreover, our network learns adaptive fusion weights via learnable projections (Eq. 4), ensuring scale-aware feature fusion for pose regression.

Normal as Approaching Prior. The orientation of a grasp pose can be defined by a combination of a view vector and an in-plane rotation angle. As demonstrated in EconomicGrasp [3], viewpoint selection significantly impacts grasp pose quality. By averaging grasp scores across various predefined views, we observe in Fig. 5 that certain viewpoints inherently lead to more accurate grasp pose regression.

Building on this observation, we propose that when the grasp pose is aligned with the normal direction of the object, a more stable grasp can be achieved. As shown in Fig.5, viewpoints within a 15° cone of the surface normal direction can on average generate high-quality grasp poses (defined as the top 1% of all grasp poses). To leverage this insight, we compute the normal vector $N \in \mathbb{R}^{N \times 3}$ for each point p_i in the point cloud $P \in \mathbb{R}^{N \times 3}$ based on its neighboring points p^{right} , p^{left} , p^{down} , and p^{up} . The normal vector n_i is obtained by taking the cross product of the horizontal tangent vector $v_h = p_{right} - p_{left}$ and the vertical tangent vector $v_v = p_{down} - p_{up}$, and then normalizing the result:

$$n_i = \frac{(p^{right} - p^{left}) \times (p^{down} - p^{up})}{|(p^{right} - p^{left}) \times (p^{down} - p^{up})|}. \quad (5)$$

Consequently, we incorporate surface normals as point features ($f_i = [x_i, n_i]$, combining position x_i and normal n_i) enhances geometric representation modeling capability, improving grasp pose prediction performance.

C. SimGraspNet dataset

Simulation Setup. We construct our simulation dataset using Isaac Sim [9]. A virtual RGB-D camera is mounted on the robotic arm’s wrist, following a predefined motion trajectory. Referring to GraspNet-1Billion [1], the collection trajectory encompasses 256 distinct viewpoints distributed over a quarter-sphere. As the robotic arm moves along this trajectory, we systematically capture RGB-D images,

object segmentation masks, camera poses relative to a fixed coordinate system, camera intrinsics, and other metadata.

Assets and Cluttered Scene. We utilize the same set of 40 objects from the GraspNet-1Billion [1] training set and enhance them with real-world physical properties such as gravity, velocity, acceleration, and mass, enabling realistic interactions. Subsequently, a subset of these objects is then randomly selected and dropped from varying heights with randomized initial positions and orientations. As they descend, the objects collide with each other and the table, resulting in diverse and naturalistic object poses. This process generates approximately 400 cluttered scenes, forming our SimGraspNet dataset. Finally, we generate ground truth labels for these scenes following the methodology proposed in GraspNet-1Billion[1].

D. Semantic Grasp

In real-world applications, grasping a user-specified object or a specific part of an object is a common requirement, such as the handle of a hammer. To enable this semantic grasping capability, we integrate the powerful VLM model with FineGrasp. As shown in Fig. 1, our framework consists of three steps: (1) a pre-trained VLM is used to identify the mask of the target object or its specific part, (2) FineGrasp generates grasp poses for the entire scene, and (3) grasp candidates are filtered, retaining only those within the semantic mask.

However, directly applying VLM models to part grounding tasks often results in suboptimal performance due to their limited fine-grained understanding of objects. To address this, we propose a coarse-to-fine processing pipeline. Given an input RGB image and instructions, we first use the VLM model to ground the target object at the object level. The identified object is then cropped from the image, allowing for fine-grained part grounding to determine the specific graspable region. This approach enables effective part grounding even in cluttered scenes. We choose Sa2VA-4B [13] for its superior performance in grounding tasks and high efficiency in terms of frames per second (FPS).

IV. EXPERIMENTS

In this section, we conduct a comprehensive experimental evaluation of FineGrasp. We begin by detailing the experimental setup, followed by a performance comparison against state-of-the-art methods. Next, we perform ablation studies to analyze the impact of each key component. Finally, extensive real-world robot experiments are conducted to validate FineGrasp’s effectiveness in grasping delicate objects and enabling semantic grasping.

A. Experiment Setup

Dataset and Metrics. We evaluate the performance of our method using the widely adopted benchmark GraspNet-1Billion, which comprises 190 cluttered scenes captured in the real-world. We utilize the original division of the dataset into training and testing subsets, consisting of 100 scenes for training. The test sets are further categorized into Seen, Similar and Novel based on the characteristics of the

objects present. The RealSense split is utilized for better depth quality. We follow the official evaluation protocol, wherein detected grasp poses are initially filtered through non-maximum suppression, followed by the evaluation of the top 50 grasp poses using the average precision (AP) metric.

Baseline comparisons. Our method is built upon the foundation of EconomicGrasp [3], with several improvements. We compare it with GraspNet-Baseline [1], Scale Balance Grasp [6], HGGD [14], GSNet [7], AnyGrasp [2], and EconomicGrasp [3].

Implementation Details. Our model is implemented using the PyTorch framework and trained on 8 Nvidia 4090 GPUs. The Adam optimizer is used, with a batch size of 4 per GPU and an initial learning rate of 0.001. The learning rate follows a cosine decay schedule with a linear warm-up strategy. The training process spans 10 epochs and takes approximately 2 hours to reach convergence.

B. Comparison with the State-of-the-art

Table I presents the comparative results of FineGrasp with other representative approaches on GraspNet-1B Dataset. Despite our focus on improving performance for delicate objects, FineGrasp outperforms other methods across Seen, Similar, and Novel settings. FineGrasp achieves an average AP of 53.97 on the RealSense split. Additionally, by incorporating collision detection, the average AP increases to 55.47, as shown in the final row of Table I.

TABLE I
EXPERIMENT ON GRASPNET-1B DATASET. SHOWING APs ON
REALSENSE SPLIT. CD MEANS COLLISION DETECTION

Method	Seen	Similar	Novel	Average
GraspNet-Baseline [1]	27.56	26.11	10.55	21.41
Scale Balanced Grasp [6]	58.95	52.97	22.63	44.85
HGGD [14]	64.45	53.59	24.59	47.54
GSNet [7]	67.12	54.80	24.31	48.74
AnyGrasp [2] + CD	66.12	56.09	24.81	49.01
EconomicGrasp [3]	68.21	61.19	25.48	51.63
FineGrasp	71.67	62.83	27.40	53.97
FineGrasp + CD	73.71	64.56	28.14	55.47

C. Ablation Studies

Grasping model. In this section, we assess the effectiveness of the proposed modules. First, to evaluate the effectiveness of our MRA module, we replace the feature fusion method with the one proposed in Scaled Balanced Grasp [6]. Additionally, we introduce a scaled metric designed to more accurately assess the scale-aware grasping quality within a scene. Specifically, the maximum width of the gripper is partitioned into three intervals: 0-4 cm for Small, 4-7 cm for Medium, and 7-10 cm for Large. Table II present the compare result, demonstrating that the proposed MRA module achieves superior performance across small, medium, and large objects.

Next, we conduct an ablation study on our proposed modules and simulation dataset, with the results summarized in Table III. The results indicate that the Instance-Norm

TABLE II
ABLATION STUDY OF MULTI-RANGE FEATURE FUSION.

Feature fusion	Small	Medium	Large	Average
MsCG [6]	15.87	50.52	55.51	40.63
MRA	16.23	50.67	56.92	41.27

Graspness module significantly improves small-scale performance, increasing it from 11.47 to 14.74. This improvement is attributed to its mitigation of the over-suppression effect caused by global normalization, allowing small-scale objects to receive more adequate learning during the point proposal stage. Furthermore, incorporating the Normal Prior module enriches point cloud features by leveraging surface orientation, thereby strengthening geometric modeling capability. This results in consistent performance gains on the Novel split in our experiments. Moreover, the mix training with our SimGraspNet dataset leads to a significant improvement in small-object performance, increasing AP from 16.23 to 18.87. This highlights the impact of depth sensor noise on small objects and demonstrates that incorporating simulation data can effectively mitigate this issue.

Simulation dataset. Table IV displays the results on our SimGraspNet dataset, wherein the EconomicGrasp is selected as the grasp model, with the sole variable being the training data. The results demonstrate that, when trained exclusively with our SimGraspNet, a satisfactory performance is attainable, namely 59.35 for Seen, 56.74 for Similar and 23.68 for Novel. To mitigate the discrepancy between simulation and reality, we introduce a Gaussian Shift to the simulated depth images to replicate real sensor noise. Furthermore, we employ an off-the-shelf depth restoration method [15] to preprocess the test depth images. The corresponding result, denoted as SimGraspNet+Sim2real, indicates a substantial reduction in the sim-to-real gap across all test sets. Moreover, when trained jointly on both simulated and real-world data, denoted as SimGraspNet+GraspNet-1B, the performance improves by 3.09, 4.29 and 0.8 respectively when compared to the baseline, thereby substantiating the efficacy of our dataset.

D. Real-World Experiment on delicate objects

We conduct a real-world experiments to validate the ability of our method, where a 7-DoF FR3 robotic arm, supplied by Franka Emika and equipped with a parallel-jaw gripper, is selected as our platform. Additionally, a RealSense D435i depth sensor is mounted on a tripod positioned in front of the arm as shown in Fig.6 (a). A total of 18 small objects were gathered to construct 5 test scenes, with each scene comprising 6 objects, as depicted in Fig.6 (b). In each trial, the robotic arm performs the grasping action associated with the highest score, and iteratively removes objects until the workspace is cleared or two failures occur in succession. If two consecutive grasp failures occur, the scene is marked as incomplete.

Table V reports the result of real robot experiments. FineGrasp achieves success and completion rates of 91%

TABLE III

THE IMPACT OF COMPONENTS IN THE PROPOSED METHOD: NP (NORMAL PRIOR), MRA (MULTI-RANGE ATTENTION), AND ING (INSTANCE-NORM GRASPNESS).

ING	MRA	NP	SimGraspNet	Seen	Similar	Novel	Average	Small	Medium	Large
✓	✓	✓	✓	68.13	59.94	25.32	51.13	11.47	48.02	53.76
				69.51	60.94	25.44	51.96	14.74	48.53	54.85
				70.32	61.40	25.45	52.39	14.33	49.94	54.82
				69.71	60.80	25.92	52.14	13.01	48.88	55.11
✓	✓	✓	✓	70.89	61.61	25.76	52.75	14.63	49.38	55.52
				70.71	61.27	26.58	52.85	15.40	50.02	55.23
✓	✓	✓	✓	71.67	62.83	27.40	53.97	16.23	50.67	56.92
✓	✓	✓	✓	70.80	63.84	26.51	53.71	18.87	50.61	56.53



(a) System setup for our real-world experiments



(b) Test object samples in the real-world grasping

Fig. 6. Robot and object settings in the real-world grasping experiments.

TABLE IV

THE EXPERIMENT ON SIMULATION DATASET

Train set	Seen	Similar	Novel
GraspNet-1B	68.13	59.94	25.32
SimGraspNet	59.35	56.74	23.68
SimGraspNet + Sim2real	62.47	58.41	24.16
SimGraspNet+GraspNet-1B	71.22	64.24	26.12

and 100%, respectively, whereas GSNet and EconomicGrasp attain only 78%/40% and 69%/20%. The substantial gap in completion rate demonstrated by our model underscores its effectiveness in handling delicate object grasps.

TABLE V

REAL-WORLD EXPERIMENT ON DELICATE OBJECTS

Scene	Objects	GSNet [7]	EconomicGrasp [3]	FineGrasp
1	6	5/6	6/6	6/6
2	6	5/6	5/6	6/7
3	6	6/8	4/6	6/6
4	6	2/6	4/6	6/6
5	6	4/6	6/8	6/8
Success Rate		69%(22/32)	78%(25/32)	91%(30/33)
Completion Rate		20%(1/5)	40%(2/5)	100%(5/5)

E. Real-World Experiments on semantic grasp

To validate our coarse-to-fine semantic grasp system, we conduct empirical grasp experiments under real-world conditions. We utilize two test settings to assess the practical semantic grasping capabilities: Object-grounding grasp and Part-grounding grasp.

TABLE VI

REAL-WORLD EXPERIMENT ON OBJECT-GROUNDING GRASP

Scene	Objects	Object Prompt	EconomicGrasp [3]	FineGrasp
1	8	Orange duck	3/3	3/3
2	9	Green box	3/3	3/3
3	12	globe	2/3	2/3
4	11	Lip balm	0/3	2/3
5	10	Metal workpiece	3/3	3/3
Success Rate			73%(11/15)	86%(13/15)

In the Object-grounding experiment, selected delicate objects are placed in a cluster scene containing 8 to 12 objects, with each object positioned randomly. The grasping is repeated three times for each scene. If semantic grounding failure occurs, the trial is excluded from the statistical results. As shown in the table VI, our method outperforms EconomicGrasp, achieving a success rate of 86%. Specially, small objects, such as lip balm, in the cluster scene are often overlooked in the point proposal stage, leading to few or no high-quality grasp poses. However, our FineGrasp method

achieves a success rate of 66% for this object, whereas EconomicGrasp fails to complete a single successful grasp.

TABLE VII
REAL-WORLD EXPERIMENT ON PART-GROUNDING GRASP

Object	Part Prompt	GSNet [7]	FineGrasp
Hand Cream	Cap of the hand cream	0/5	4/5
Cup	Handle of the cup	5/5	3/5
Crane	Arm of the crane	4/5	5/5
Tiger	Head of the tiger	4/5	5/5
Pliers	Left handle of the pliers	1/5	4/5
Success Rate		56%(14/25)	84%(21/25)

In the Part-grounding grasp setting, we collect 5 objects, each featuring distinct parts, such as cup and pliers, and place them randomly with various orientations. Given a specific instruction, such as "the handle of the cup", 5 attempts were made accordingly. Note that a trial was deemed successful only if the specified part of the object was grasped. As shown in Table VII, our approach attained an average success rate of 84%, demonstrating the potential of integrating FineGrasp into downstream manipulation applications.

V. CONCLUSIONS

In this work, we propose FineGrasp, a novel method that enhances grasp pose estimation for fine objects through improved label normalization, multi-range attention, normal prior, and mixed training with simulated data. These innovations address key challenges in delicate object grasping, leading to more accurate and robust predictions. Beyond improving grasp performance, our approach eliminates the need for segmentation during inference and offers a more data-efficient training strategy. This work contributes to advancing robotic grasping in cluttered and unstructured environments. Future work could expand simulation scenarios for small and articulated objects to further enhance generalization and robustness of grasp model.

REFERENCES

- [1] H.-S. Fang, C. Wang, M. Gou, and C. Lu, "Graspnet-1billion: A large-scale benchmark for general object grasping," in *Proceedings of the IEEE/CVF conference on computer vision and pattern recognition*, 2020, pp. 11 444–11 453.
- [2] H.-S. Fang, C. Wang, H. Fang, M. Gou, J. Liu, H. Yan, W. Liu, Y. Xie, and C. Lu, "Anygrasp: Robust and efficient grasp perception in spatial and temporal domains," *IEEE Transactions on Robotics*, vol. 39, no. 5, pp. 3929–3945, 2023.
- [3] X.-M. Wu, J.-F. Cai, J.-J. Jiang, D. Zheng, Y.-L. Wei, and W.-S. Zheng, "An economic framework for 6-dof grasp detection," in *European Conference on Computer Vision*. Springer, 2024, pp. 357–375.
- [4] H. Huang, F. Lin, Y. Hu, S. Wang, and Y. Gao, "Copa: General robotic manipulation through spatial constraints of parts with foundation models," in *2024 IEEE/RSJ International Conference on Intelligent Robots and Systems (IROS)*. IEEE, 2024, pp. 9488–9495.
- [5] Y. Qian, X. Zhu, O. Biza, S. Jiang, L. Zhao, H. Huang, Y. Qi, and R. Platt, "Thinkgrasp: A vision-language system for strategic part grasping in clutter," *arXiv preprint arXiv:2407.11298*, 2024.
- [6] M. Haoxiang and D. Huang, "Towards scale balanced 6-dof grasp detection in cluttered scenes," in *Conference on Robot Learning (CoRL)*, 2022.
- [7] C. Wang, H.-S. Fang, M. Gou, H. Fang, J. Gao, and C. Lu, "Graspness discovery in clutters for fast and accurate grasp detection," in *Proceedings of the IEEE/CVF International Conference on Computer Vision*, 2021, pp. 15 964–15 973.
- [8] J. Li and D. J. Cappelleri, "Sim-grasp: Learning 6-dof grasp policies for cluttered environments using a synthetic benchmark," *IEEE Robotics and Automation Letters*, 2024.
- [9] J. Liang, V. Makovychuk, A. Handa, N. Chentanez, M. Macklin, and D. Fox, "Gpu-accelerated robotic simulation for distributed reinforcement learning," in *Conference on Robot Learning*. PMLR, 2018, pp. 270–282.
- [10] J. Zhang, H. Liu, D. Li, X. Yu, H. Geng, Y. Ding, J. Chen, and H. Wang, "Dexgraspnet 2.0: Learning generative dexterous grasping in large-scale synthetic cluttered scenes," in *8th Annual Conference on Robot Learning*, 2024.
- [11] P. Liu, Y. Orru, J. Vakil, C. Paxton, N. M. M. Shafiullah, and L. Pinto, "Ok-robot: What really matters in integrating open-knowledge models for robotics," *arXiv preprint arXiv:2401.12202*, 2024.
- [12] M. Pan, J. Zhang, T. Wu, Y. Zhao, W. Gao, and H. Dong, "Omnimanip: Towards general robotic manipulation via object-centric interaction primitives as spatial constraints," *arXiv preprint arXiv:2501.03841*, 2025.
- [13] H. Yuan, X. Li, T. Zhang, Z. Huang, S. Xu, S. Ji, Y. Tong, L. Qi, J. Feng, and M.-H. Yang, "Sa2va: Marrying sam2 with llava for dense grounded understanding of images and videos," *arXiv preprint arXiv:2501.04001*, 2025.
- [14] S. Chen, W. Tang, P. Xie, W. Yang, and G. Wang, "Efficient heatmap-guided 6-dof grasp detection in cluttered scenes," *IEEE Robotics and Automation Letters*, vol. 8, no. 8, pp. 4895–4902, 2023.
- [15] L. Yang, B. Kang, Z. Huang, Z. Zhao, X. Xu, J. Feng, and H. Zhao, "Depth anything v2," *Advances in Neural Information Processing Systems*, vol. 37, pp. 21 875–21 911, 2025.